Optimized Cosine-Modulated Filter Banks Using the Frequency Response Masking Approach

Miguel B. Furtado Jr., Sergio L. Netto, and Paulo S. R. Diniz
Universidade Federal do Rio de Janeiro

Abstract— **An optimization procedure for cosine-modulated filter banks (CMFB) using the frequency-response masking approach is proposed. In the given method, we perform minimization of the maximum attenuation level in the filter's stopband, subject to intersymbol interference (ISI) and intercarrier interference (ICI) constraints. For optimization, a quasi-Newton algorithm with line search is used, and we propose a simplified analytical expressions to impose the interference constraints. The result is lower levels of ISI and ICI for a pre-determined filter order, or reduced filter complexity for given levels of interferences.**

I. Introduction

Cosine-modulated filter banks (CMFBs) are commonly used in practice due to two main features [6], [1]: First, their realization relies only on the design of a single prototype filter; Second, they have computationally efficient implementations based on fast algorithms for the discrete cosine transform (DCT). For very demanding applications where maximum selectivity is required, the prototype filter for the CMFB tends to present very high order, thus increasing the computational complexity of the overall structure. A possible design procedure that avoids this problem is to use the FRM approach [5] for designing the CMFB prototype filter. This technique is known to produce sharp linear-phase FIR filters with reduced number of coefficients, resulting in the so-called FRM-CMFB structure [3].

This paper presents an optimization procedure of the FRM-CMFB prototype filter aiming at the reduction of the stopband maximum magnitude, with constraints on the intersymbol interference (ISI) and intercarrier interference (ICI) of the overall structure. It is then verified that the reduced number of coefficients required by the FRM approach not only generates a more efficient structure in terms of computational complexity, but it also leads to a simpler and faster optimization problem. The optimization procedure is based on variations of sequential quadratic programming, using a constrained quasi-Newton method with line search. A simplified analytical derivation of the interference constraints is given, which greatly speeds up the optimization procedure. The results include lower levels of ISI and ICI for a fixed filter order, or reduced filter bank complexity for given levels interferences.

The remaining of the paper is organized as follows: In Section 2, descriptions of the CMFB structure and the transmultiplexer (TMUX) configuration are given. In Section 3, a brief explanation of the FRM approach for designing low-complexity FIR filters is provided. In Section 4, the FRM-CMFB implementation is then presented as a computationally efficient alternative to design highly selective filter banks. In Section 5, the optimization procedure for the FRM-CMFB prototype filter is presented with emphasis given on a simplified analytical derivation for the interference constraints. Then, Section 6 includes some design examples, showing improved results achieved with the optimized FRM-CMFB structure.

Programa de Engenharia Elétrica-COPPE/EE/UFRJ, PO Box 68504, Rio de Janeiro, RJ, 21945-970, BRAZIL. E-mails: {furtado, sergioln, diniz}@lps.ufrj.br

II. The CMFB and TMUX Systems

CMFBs are easy-to-implement structures based on a single prototype filter, whose modulated versions will form the analysis and synthesis subfilters of the complete bank [7]. The modulation operation is implemented in an efficient manner by using fast algorithms for the DCT. Usually, the prototype filter for M-band filter bank is specified by its 3 dB attenuation point and the stopband edge at frequencies

$$\omega_{3dB} \approx \frac{\pi}{2M}; \quad \omega_s = \frac{(1+\rho)\pi}{2M} \tag{1}$$

respectively, where ρ is the so-called roll-off factor.

Assuming that the prototype filter has an impulse response $h_p(n)$ of order N_p, its transfer function is expressed as

$$H_p(z) = \sum_{n=0}^{N_p} h_p(n) z^{-n} \tag{2}$$

The impulse response of the analysis and synthesis subfilters are then described by

$$h_m(n) = h_p(n) c_{m,n} \tag{3}$$

$$f_m(n) = h_p(n) \bar{c}_{m,n} \tag{4}$$

for $m = 0, 1, \ldots, (M-1)$ and $n = 0, 1, \ldots, N_p$, where

$$c_{m,n} = 2\cos\left[\frac{(2m+1)(n-N_p/2)\pi}{2M} + (-1)^m \frac{\pi}{4}\right] \tag{5}$$

$$\bar{c}_{m,n} = 2\cos\left[\frac{(2m+1)(n-N_p/2)\pi}{2M} - (-1)^m \frac{\pi}{4}\right] \tag{6}$$

If the prototype filter has $(N_p+1) = 2KM$ coefficients, then it can be decomposed into $2M$ polyphase components

$$H_p(z) = \sum_{j=0}^{2M-1} z^{-j} E_j(z^{2M}) \tag{7}$$

with $E_j(z)$, for $j = 0, 1, \ldots, (2M-1)$, given by

$$E_j(z) = \sum_{k=0}^{K-1} h_p(2kM + j) z^{-k} \tag{8}$$

Therefore, using the fact that $c_{m,(n+2kM)} = (-1)^k c_{m,n}$, the analysis filter can be written as

$$H_m(z) = \sum_{j=0}^{2M-1} c_{m,j} z^{-j} E_j(-z^{2M}) \tag{9}$$

With this polyphase decomposition, it can be shown that all filtering operations can be performed using sparse matrix multiplications involving an identity matrix, a reversed identity matrix, and a DCT-IV operation, leading to a reduced number of operations per output sample [7].

Figure 1 shows the block diagram of the filter bank described above, whose input-output relation is described by

$$\hat{Y}(z) = \frac{1}{M}\left[T_0(z)Y(z) + \sum_{i=1}^{M-1} T_i(z)Y(ze^{\frac{j2\pi i}{M}})\right] \quad (10)$$

The first term in equation (10), $T_0(z)$, is the direct transfer function and must be the unique term in an alias-free design, which includes the perfect reconstruction (PR) filter bank, as a particular case. The second term, involving all other $T_i(z)$, is the aliasing transfer function, which quantifies the influences in a given band from all other bands. These terms are expressed by

$$T_0(z) = \sum_{m=0}^{M-1} F_m(z)H_m(z) \quad (11)$$

$$T_i(z) = \sum_{m=0}^{M-1} F_m(z)H_m(ze^{\frac{-j2\pi i}{M}}) \quad (12)$$

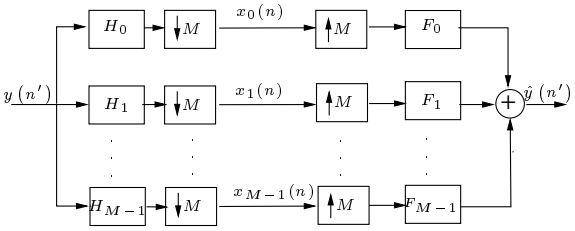

Fig. 1. M-channel maximally decimated filter bank.

The maximally decimated M-channel TMUX system is a filter bank where the analysis and synthesis blocks are switched, in order to form a system with M input/output channels, as depicted in Figure 2 [7]. This structure interpolates and filter each input signal, adding the resulting signals on each branch to form a single signal for transmission over a given channel C. At the receiver, the signal is then split back into M-channels to generate the desired M outputs. The design problem of such system can be simplified by assuming that the channel response is ideal ($C \equiv 1$), or a pure delay. Then, in the PR case, each output signal is identical to its equivalent input, whereas in the nearly-PR (NPR), a small interference among the sub-channels is present.

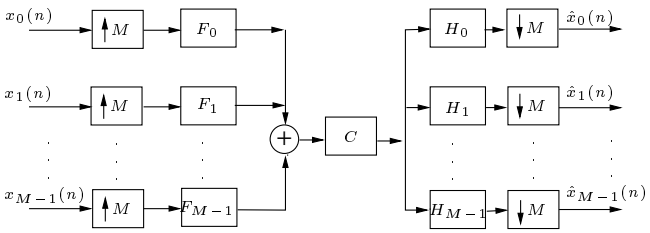

Fig. 2. M-channel maximally decimated TMUX system.

The general relation that describes the transfer functions of the TMUX system is

$$\hat{\mathbf{x}}(z^M) = \frac{1}{M}\mathbf{T}(\mathbf{z^M})\mathbf{x}(\mathbf{z^M}) \quad (13)$$

where

$$\hat{\mathbf{x}}(z) = [\hat{X}_0(z)\ \hat{X}_1(z)\ \ldots\ \hat{X}_{M-1}(z)]^T \quad (14)$$

$$\mathbf{x}(\mathbf{z}) = [\mathbf{X_0}(\mathbf{z})\ \mathbf{X_1}(\mathbf{z})\ \ldots\ \mathbf{X_{M-1}}(\mathbf{z})]^{\mathbf{T}} \quad (15)$$

and

$$[\mathbf{T}(\mathbf{z^M})]_{\mathbf{ab}} = \sum_{\mathbf{m=0}}^{\mathbf{M-1}} \mathbf{H_a}(\mathbf{ze}^{-\frac{\mathbf{j2\pi m}}{\mathbf{M}}})\mathbf{F_b}(\mathbf{ze}^{-\frac{\mathbf{j2\pi m}}{\mathbf{M}}}) \quad (16)$$

for $a, b = 0, 1, \ldots, (M-1)$. The matrix $\mathbf{T}(\mathbf{z^M})$ is the so-called transfer matrix whose elements, $[\mathbf{T}(\mathbf{z^M})]_{\mathbf{ab}}$, represent the transfer function between the interpolated input a and the decimated output b. Thus, the main diagonal entries of this matrix, $[\mathbf{T}(\mathbf{z^M})]_{\mathbf{aa}}$ represent the transfer functions of each channel, and the other terms give the crosstalk between two different channels. In the NPR case, no restrictions apply to the transfer matrix, whereas in the PR case, the crosstalk terms must be zero and the diagonal terms become simple delays [1].

In a TMUX system, one would be interested in estimating the total ISI and ICI figures of merit which are given by [1]:

$$\text{ISI} = \max_a \left\{ \sum_n [\delta(n) - t_a(n)]^2 \right\} \quad (17)$$

$$\text{ICI} = \max_{a,\omega} \left\{ \sum_{b=0, a\neq b}^{M-1} |[\mathbf{T}(\mathbf{e^{j\omega}})]_{\mathbf{ab}}|^{\mathbf{2}} \right\} \quad (18)$$

where $\delta(n)$ is the ideal impulse, $t_a(n)$ is the impulse response for the ath channel, and the term $[\mathbf{T}(\mathbf{e^{j\omega}})]_{\mathbf{ab}}$ is the crosstalk between the ath and bth channels, whose expression is given by equation (16).

III. The FRM Approach

The basic principle behind the FRM approach consists of the usage of a complementary pair of interpolated linear-phase FIR filters. The base filter, $H_b(z)$, and its complementary version, $H_{b_c}(z)$ are interpolated by a factor of L, to form sharp transition bands, at the cost of introducing multiple passbands on each frequency response. These repetitive passbands are then filtered out by the so-called positive and negative masking filters, $G_m(z)$ and $G_{m_c}(z)$ respectively, and added together to compose the overall desired filter, $H_f(z)$. This whole procedure is illustrated in Figure 3. In practice, L is chosen in a heuristic way such that the total number of coefficients of the overall FRM filter is minimized. The subfilters can still be optimized depending on the application, as described in [4], [2].

IV. The FRM-CMFB Structure

From the analysis of the FRM and the CMFB schemes, an efficient FRM-CMFB joint structure can be derived if the interpolator factor L for the FRM filter can be written as [3]

$$L = 2K_aM + \frac{M}{K_b} \quad (19)$$

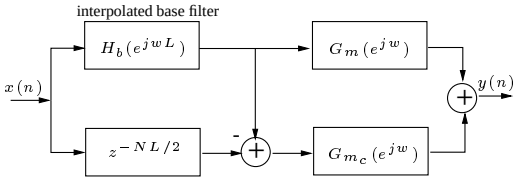

Fig. 3. FRM structure: The interpolated complementary pair of filters and the respective masking filters work together to produce the desired frequency response.

with $K_a \geq 0$ and $K_b > 0$ being integer numbers. In such case, using solely the upper branch on the FRM scheme, the mth analysis filter can be written as

$$H_m(z) = \sum_{i=0}^{N_b} \left[h_b(i) z^{-Li} \sum_{n=0}^{N_m} c_{m,[n+Li]} g_1(n) z^{-n} \right] \quad (20)$$

where N_m is the order and $g_1(n)$ are the coefficients of the masking filter. Notice that for the general FRM structure, a similar description should be obtained for the lower branch, and the results for both branches added together. Hence, from equation (20), by using $Q = 2K_b$ polyphase components for the base filter, with $i = kQ + q$ and $(N_b + 1) = QK_c$, we have, after some manipulations, that

$$H_m(z) = \sum_{q=0}^{Q-1} \sum_{k=0}^{K_c-1} \left[h_b(kQ+q) z^{-L(kQ+q)} \times (-1)^{(k+K_a q)} \sum_{n=0}^{N_m} c_{m,(n+\frac{M}{K_b}q)} g_1(n) z^{-j} \right] \quad (21)$$

By writing the modified polyphase components of the interpolated base filter

$$H'_{b1q}(z) = \sum_{k=0}^{K_c-1} (-1)^{K_a q} h_b(kQ+q) z^{-k} \quad (22)$$

for $q = 0, 1, \ldots, (Q-1)$, and by using the masking filter polyphase component

$$E'_j(z) = \sum_{k=0}^{K_d-1} g_1(2kM + j) z^{-k} \quad (23)$$

for $j = 0, 1, \ldots, (2M-1)$, equation (21) becomes

$$H_m(z) = \sum_{q=0}^{Q-1} \left[z^{-Lq} H'_{b1q}(-z^{LQ}) \times \sum_{j=0}^{2M-1} c_{m,(n+\frac{M}{K_b}q)} z^{-j} E'_j(-z^{2M}) \right] \quad (24)$$

This relation leads to the structure depicted in Figure 4, where the value of K is equivalent to the CMFB case (see equation (8)).

V. Optimized FRM-CMFB

Standard optimization goals for the CMFB prototype filter are to minimize the objective functions

$$E_2 = \int_{\omega_r}^{\pi} |H_p(e^{j\omega})|^2 d\omega \quad (25)$$

$$E_\infty = \max_{\omega \in [\omega_r, \pi]} |H_p(e^{j\omega})| \quad (26)$$

which correspond to the total energy and the maximum magnitude value in the filter's stopband, respectively, with ω_r being the stopband edge frequency. In practice, to control the aliasing distortion and the overall direct transfer of the filter bank, the following constraints are introduced

$$1 - \delta_1 \leq |T_0(e^{j\omega})| \leq 1 + \delta_1 \quad (27)$$

$$|T_i(e^{j\omega})| \leq \delta_2 \quad (28)$$

for $i = 1, 2, \ldots, (M-1)$ and $\omega = \in [0, \pi]$.

In the FRM-CMFB structure, the prototype filter $H_p(z)$ is as given in Figure 3, and the approximation problem resides on finding a base filter, a positive masking filter (upper branch), and a negative masking filter (lower branch) that optimize E_2 or E_∞ subject to the constraints given by equations (27) and (28). In this work, for the optimization we used a quasi-Newton algorithm with line search implemented with the command `fmincon` in MATLAB® [8]. The gradient vector was determined analytically to reduce computational burden during optimization procedure. The functions $T_0(z)$ and $T_i(z)$, for $i = 1, 2, \ldots, (M-1)$, required to impose the desired constraints, have extremely high computational complexity. Some simplifications, however, can significantly simplify the problem of evaluating these constraints, as described below.

In the z domain, equations (3) and (4) become [7]

$$H_m(z) = \alpha_m \beta_m H_p(z e^{\frac{-j(2m+1)\pi}{2M}}) + \alpha_m^* \beta_m^* H_p(z e^{\frac{j(2m+1)\pi}{2M}}) \quad (29)$$

$$F_m(z) = \alpha_m^* \beta_m H_p(z e^{\frac{-j(2m+1)\pi}{2M}}) + \alpha_m \beta_m^* H_p(z e^{\frac{j(2m+1)\pi}{2M}}) \quad (30)$$

for $m = 0, 1, \ldots, (M-1)$, where

$$\alpha_m = e^{\frac{j(-1)^m \pi}{4}}; \quad \beta_m = e^{\frac{-jN_p(2m+1)\pi}{4M}} \quad (31)$$

where N_p is the prototype filter order. Using these relations in equation (11), we get

$$T_0(z) = \sum_{m=0}^{M-1} \left({\beta_m}^2 H_p^2(z e^{\frac{-j(2m+1)\pi}{2M}}) + {\beta_m^*}^2 H_p^2(z e^{\frac{j(2m+1)\pi}{2M}}) \right) \quad (32)$$

since $({\alpha_m}^2 + {\alpha_m^*}^2) = 0$ and $\alpha_m \alpha_m^* = 1$, for all m.

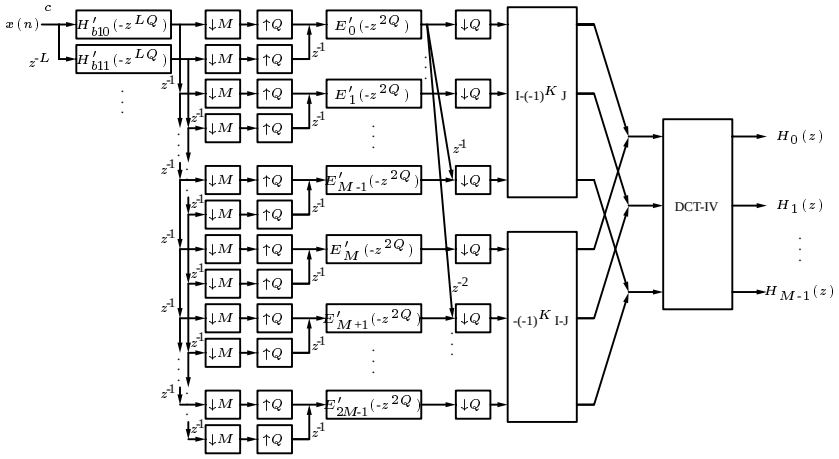

Fig. 4. CMFB structure using FRM for the general case of $L = 2K_aM + \frac{M}{K_b}$.

Using $H_p(z)$ as defined in equation (2), we obtain

$$\begin{aligned}
T_0(z) &= \sum_{m=0}^{M-1} {\beta_m}^2 \left(\sum_{n=0}^{N_p} h_p(n) z^{-n} e^{\frac{j(2m+1)\pi n}{2M}} \right)^2 + \\
&\quad \sum_{m=0}^{M-1} {\beta_m^*}^2 \left(\sum_{n=0}^{N_p} h_p(n) z^{-n} e^{\frac{-j(2m+1)\pi n}{2M}} \right)^2 \\
&= \sum_{m=0}^{M-1} {\beta_m}^2 \left(\sum_{n=0}^{2N_p-1} a(n) z^{-n} e^{\frac{j(2m+1)\pi n}{2M}} \right) + \\
&\quad \sum_{m=0}^{M-1} {\beta_m^*}^2 \left(\sum_{n=0}^{2N_p-1} a(n) z^{-n} e^{\frac{-j(2m+1)\pi n}{2M}} \right) \\
&= \sum_{n=0}^{2N_p-1} a(n) z^{-n} \times \\
&\quad \left[\sum_{m=0}^{M-1} \left({\beta_m}^2 e^{\frac{j(2m+1)\pi n}{2M}} + {\beta_m^*}^2 e^{\frac{-j(2m+1)\pi n}{2M}} \right) \right] \\
&= \sum_{n=0}^{2N_p-1} a(n) z^{-n} \gamma(n) \qquad (33)
\end{aligned}$$

where the coefficients $a(n)$ result from the convolution of $h_p(n)$ with itself, that is

$$Z\{h_p(n) * h_p(n)\} = \sum_{n=0}^{2N_p-1} a(n) z^{-n} \qquad (34)$$

and $\gamma(n)$ is defined as

$$\gamma(n) = \begin{cases} 2M(-1)^c, & \text{for } (N_p - n) = 2Mc,\ c \text{ integer} \\ 0, & \text{otherwise} \end{cases} \qquad (35)$$

Similarly, all functions $T_i(z)$ can be evaluated using this simplification, by modulating one of the terms of the convolution in equation (34), as follows:

$$T_i(z) = Z\left\{ \left(e^{\frac{j2\pi in}{M}} h_p(n) * h_p(n) \right) \gamma(n) \right\} \qquad (36)$$

for $i = 1, 2, \ldots, (M-1)$. Due to the symmetry in the modulation function, $T_i(z) = T_{M-i}(z)$. Hence, one may evaluate functions $T_i(z)$ only for $i = 1, 2, \ldots, \lfloor M/2 \rfloor$, where the operator $\lfloor x \rfloor$ denotes the integer part of x.

VI. Design Examples

A quasi-Newton algorithm with line search was applied on both direct-form (standard equiripple filter) and FRM realizations of the CMFB prototype filter aiming to achieve improved performances with respect to E_∞ given in equation (26). The prototype filters were used on a TMUX system, and the parameters of interest of this structure, namely passband ripple, δ_1, aliasing interference, δ_2, minimum stopband attenuation, A_r, intersymbol interference (ISI), and intercarrier interference (ICI), were measured in each case.

Example 1: The example compares the realization of a CMFB with $M = 8$ bands and $\rho = 1$, based on both direct and FRM implementations. The overall order of the prototype filters in both cases was set to $N_p = 2KM - 1 = 95$, resulting in a factor of $K = 6$ for the polyphase decomposition. The direct-form realization was optimized in [1], and its final characteristics are included in Table I. The FRM structure was developed with an interpolation factor $L = 4$, thus allowing one to discard the lower branch of the FRM diagram. The orders of the base and positive masking filters were $N_b = 18$ and $N_m = 23$, respectively, yielding an overall order of $N_p = LN_b + N_m = 95$ for the FRM filter.

Table I summarizes the results achieved by the optimization of the CMFB prototype filter. The magnitude responses of both the optimized FRM prototype filter and the complete FRM-CMFB are presented in Figures 5 and 6, respectively.

TABLE I

Figures of merit for the optimized direct-form and FRM prototype filters in Example 1.

Figures of Merit	Direct Form	FRM
# coefficients	48	22
δ_1	0.001	0.00087
δ_2 (dB)	-83.6	-88.2
A_r (dB)	-74.0	-77.4
ISI (dB)	-62.0	-63.1
ICI (dB)	-80.4	-82.0

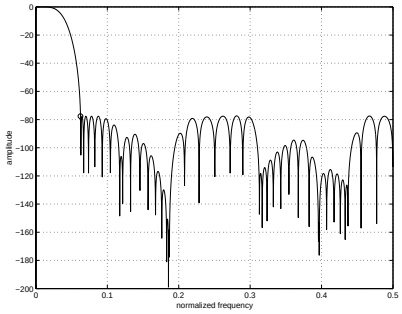

Fig. 5. Magnitude response of optimized FRM prototype filter in Example 1.

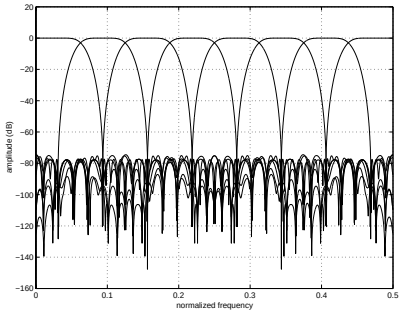

Fig. 6. Magnitude response of optimized FRM-CMFB in Example 1.

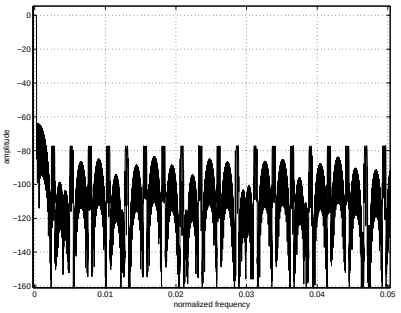

Fig. 7. Magnitude response of optimized FRM prototype filter in Example 2.

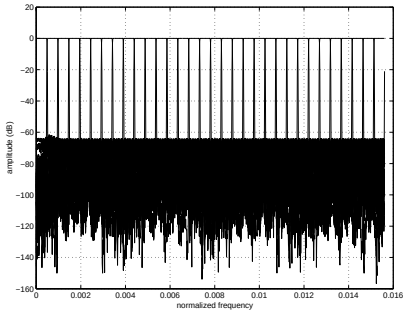

Fig. 8. Partial magnitude response (32 bands out of 1024) of optimized FRM-CMFB in Example 2.

Example 2: The example is based on a filter bank with $M = 1024$ and $\rho = 0.1$. The desired stopband attenuation is $A_r = -60dB$. These characteristics lead to a prototype filter that is unfeasible to design using the direct-form realization with standard approximation routines. So, in this exanple, we compare the optimized FRM-CMFB with its non-optimized version. In both cases, the FRM prototype filter was characterized by $N_b = 234$, $L = 384$, and $N_m = 1653$, yielding an overall filter order $N_p = 91509$ and a total of $N = 945$ distinct coefficients to be optimized. Table II shows the results of this optimization process.

TABLE II

FIGURES OF MERIT FOR THE STANDARD AND OPTIMIZED FRM PROTOTYPE FILTERS IN EXAMPLE 2.

Figures of Merit	FRM	Optimized FRM
# coefficients	945	945
δ_1	0.004	0.004
δ_2 (dB)	-60.6	-64.4
A_r (dB)	-63.8	-67.6
ISI (dB)	-123.2	-126.4
ICI (dB)	-121.2	-124.9

Figure 7 shows the optimized prototype filter in a reduced grid of frequencies (a tenth of the original) for better visualization, whereas Figure 8 depicts 32 out of the 1024 bands of the optimized FRM-CMFB in this example.

VII. CONCLUSIONS

A new design procedure for optimizing the prototype filter of a cosine-modulated filter bank (CMFB) was presented. The new method is based on the usage of a prototype filter designed with the frequency-response masking (FRM) approach, thus constituting the so-called FRM-CMFB structure. A quasi-Newton method with line search is used to perform minimization of the maximum value of the magnitude response within the filter's stopband. Other objective functions, such as filter's total stopband energy, may be considered in a similar fashion. Constraints related to intersymbol and intercarrier interferences are considered, in an extremely simplified manner, in a transmultiplexer configuration. The result is a numerically robust optimization procedure that yields very efficient filter banks with respect to several figures of merit, including the number of coefficients capitalized by the FRM-CMFB structure.

REFERENCES

[1] J. Alhava and A. Viholainen, Implementation of nearly-perfect reconstruction cosine-modulated filter banks, Proc. FinSig, 222–226, Oulu, Finland, 1999.

[2] L. C. R. de Barcellos, S. L. Netto, and P. S. R. Diniz, Design of FIR filters combining the frequency-response masking and the WLS-Chebyshev approaches, Proc. IEEE Int. Symp. Circuits and Systems, II, 613–616, Sydney, Australia, May 2001.

[3] P. S. R. Diniz, L. C. R. de Barcellos, and S. L. Netto, Design of cosine-modulated filter bank prototype filters using the frequency-response masking approach, Proc. IEEE Int. Conf. Acoustics, Speech, and Signal Processing, VI, P4.6 1–4, Salt Lake City, UT, May 2001.

[4] P. S. R. Diniz and S. L. Netto, On WLS-Chebyshev FIR digital filters, Jrnl. Circuits, Systems and Computers, 9, 155–168, 1999.

[5] Y.-C. Lim, Frequency-response masking approach for the synthesis of sharp linear phase digital filters, IEEE Trans. Circuits and Systems, CAS-33, 357–364, Apr. 1986.

[6] T. Saramäki, A generalized class of cosine-modulated filter banks, Proc. TICSP Workshop on Transforms and Filter Banks, 336–365, Tampere, Finland, June 1998.

[7] P. P. Vaidyanathan, Multirate Systems and Filter Banks, Prentice Hall, Englewood Cliffs, NJ, 1993.

[8] MATLAB Optimization Toolbox: User's Guide, The MathWorks Inc., 1997.